Differential Protein Expression Marks the Transition From Infection With *Opisthorchis viverrini* to Cholangiocarcinoma*[S]

Jarinya Khoontawad‡§¶, Chawalit Pairojkul§‖, Rucksak Rucksaken, Porntip Pinlaor§‡‡, Chaisiri Wongkham§§§, Puangrat Yongvanit§§§, Ake Pugkhem§¶¶, Alun Jones‖‖‖, Jordan Plieskatt[ab], Jeremy Potriquet[c], Jeffery Bethony[ab], Somchai Pinlaor‡§[f], and Jason Mulvenna[cdef]**

Parts of Southeast Asia have the highest incidence of intrahepatic cholangiocarcinoma (CCA) in the world because of infection by the liver fluke *Opisthorchis viverrini* (Ov). Ov-associated CCA is the culmination of chronic Ov-infection, with the persistent production of the growth factors and cytokines associated with persistent inflammation, which can endure for years in Ov-infected individuals prior to transitioning to CCA. Isobaric labeling and tandem mass spectrometry of liver tissue from a hamster model of CCA was used to compare protein expression profiles from inflammed tissue (Ovinfected but not cancerous) *versus* cancerous tissue (Ov-induced CCA). Immunohistochemistry and immunoblotting were used to verify dysregulated proteins in the animal model and in human tissue. We identified 154 dysregulated proteins that marked the transition from Ov-infection to Ov-induced CCA, *i.e.* proteins dysregulated during carcinogenesis but not Ov-infection. The verification of dysregulated proteins in resected liver tissue from humans with Ov-associated CCA showed the numerous parallels in protein dysregulation between human and animal models of Ov-induced CCA. To identify potential circulating markers for CCA, dysregulated proteins were compared with proteins isolated from exosomes secreted by a human CCA cell line (KKU055) and 27 proteins were identified as dysregulated in CCA and present in exosomes. These data form the basis of potential diagnostic biomarkers for human Ov-associated CCA. The profile of protein dysregulation observed during chronic Ovinfection and then in Ov-induced CCA provides insight into the etiology of an infection-induced inflammation-related cancer. *Molecular & Cellular Proteomics 16: 10.1074/mcp.M116.064576, 911–923, 2017.*

From the ‡Department of Parasitology, Faculty of Medicine, Khon Kaen University, Khon Kaen 40002, Thailand; §Liver Fluke and Cholangiocarcinoma Research Center, Faculty of Medicine, Khon Kaen University, Khon Kaen 40002, Thailand; ¶Department of Thai Traditional Medicine, Faculty of Natural Resources, Rajamangala University of Technology Isan, SakonNakhon Campus; ‖Department of Pathology, Faculty of Medicine, Khon Kaen University, Khon Kaen 40002, Thailand; **Department of Veterinary Technology, Faculty of Veterinary Technology, Kasetsart University, Bangkok 10900, Thailand; ‡‡Centre for Research and Development in Medical Diagnostic Laboratory, Faculty of Associated Medical Sciences, Khon Kaen University, Khon Kaen 40002, Thailand; §§Department of Biochemistry, Faculty of Medicine, Khon Kaen University, Khon Kaen 40002, Thailand; ¶¶Department of Surgery, Faculty of Medicine, Khon Kaen University, Khon Kaen 40002, Thailand; ‖‖‖The University of Queensland, Institute for Molecular Bioscience, Brisbane, QLD 4072, Australia; [a]Department of Microbiology, Immunology and Tropical Medicine, School of Medicine and Health Sciences, George Washington University, Washington, DC 20052; [b]Research Center for Neglected Diseases of Poverty, School of Medicine and Health Sciences, George Washington University, Washington, DC 20052; [c]QIMR Berghofer Medical Research Institute, Infectious Disease Program, Brisbane 4006, Australia; [d]The University of Queensland, School of Biomedical Sciences, Brisbane 4072, Australia

Received October 9, 2016, and in revised form, February 21, 2017
Published, MCP Papers in Press, February 23, 2017, DOI 10.1074/mcp.M116.064576

Author contributions: J. Potriquet, J.B., S.P., and J.M. designed research; J.K., R.R., P.P., A.P., A.J., J. Plieskatt, J. Potriquet, and J.M. performed research; J.M. contributed new reagents or analytic tools; J.K., C.P., C.W., P.Y., J.B., and J.M. analyzed data; J.K., C.P., J.B., S.P., and J.M. wrote the paper.

Although a rare cancer worldwide (0.5 per 100,000 in the USA), intrahepatic cholangiocarcinoma (CCA)[1] has the highest incidence in the world (96 per 100,000 in Northeastern Thailand (1)) in areas of the Greater Mekong subregion of Southeast Asia that overlap with transmission of the food-borne parasite *Opisthorchis viverrini* (Ov). As experimental and epidemiological evidence strongly implicate infection with this food borne pathogen in the development of CCA, Ov is

[1] The abbreviations used are: CCA, cholangiocarcinoma; APF, advanced periductal fibrosis; DAB, diaminobenzidine; DPBS, Dulbecco's PBS; IARC, International Agency for Research on Cancer; IDA, information dependent acquisition; IHC, immunohistochemistry; iTRAQ, isobaric tags for relative and absolute quantitation; OGE, OFFGEL electrophoresis; Ov, Opisthorchis viverrini; PBS, phosphate buffered saline; PBST, phosphate buffered saline tween-20; PVDF, polyvinylidene difluoride; NDMA, N-nitrosodimethylamine; MMTS, methyl methanethiosulfonate; TMA, tissue microarray; TPP, Trans Proteomic Pipeline; TEAB, triethylammonium bicarbonate.

one of only three eukaryotic pathogens considered Group 1 carcinogens by the International Agency for Research on Cancer (IARC) (2). Ov infection occurs during the consumption of undercooked fish containing the encysted metacercarial stage of the parasite (3). After ingestion of metacercaria, the parasites excyst and migrate to the intrahepatic bile duct to mature and remain patent for decades, causing prolonged mechanical, toxicological and immunopathological damage to the biliary epithelium of the host. The pathological consequences of chronic Ov infection occur primarily in the intrahepatic bile ducts (4), where CCA also arises. The location of Ov-associated CCA makes early diagnosis difficult (5), with individuals presenting late and usually because of nonspecific symptoms. Thus, despite being a slow growing tumor, Ov-associated CCA is commonly diagnosed at an advanced stage, when the primary cancer is no longer amenable to surgical extirpation and has metastasized to other organs (4). The median survival rate for individuals after diagnosis is less than 24 months, highlighting the urgent need for diagnostic markers for Ov-associated CCA.

Although the etiology of Ov-associated CCA is multi-factorial, it is clear that the chronic inflammation and prolonged immunopathology associated with chronic Ov infection are key underlying processes in the transition to CCA (6). As determined from our human studies in Ov endemic areas (4), Ov-associated CCA is the culmination of a series of clearly defined clinical and subclinical events caused by the persistent production of the growth factors and cytokines associated with chronic inflammation, would healing, and fibrogenesis (4, 7, 8). The continuous accumulation of desmoplastic (fibrotic) elements along the intrahepatic biliary tract leads to advanced periductal fibrosis (APF) and then, in some cases, to CCA (4). In this regard, Ov-associated CCA is not greatly different from other infection related cancers that induce a chronic inflammation that culminates in cancer: *e.g.* hepatocellular fibrosis and hepatocellular carcinoma from Hepatitis B and Hepatitis C viral infection (9, 10). The progression from Ov infection to CCA can be observed in a robust Syrian hamster model that uses sub-carcinogenic levels of dietary *N*-nitrosodimethylamine (NDMA) to accelerate the onset of CCA. Hamsters that are infected with Ov and fed a diet supplemented with NDMA progress to CCA whereas those that are infected with Ov but do not receive NDMA do not progress to CCA during a six month animal trial (11). In this animal model of CCA, the biliary epithelium of the hamster is markedly inflamed and displays fibrosis advancing along its length after 12 weeks of infection (12), with this is fibrotic deposition routinely present at the biliary epithelium that leads to CCA (8, 13).

In the current study, isobaric labeling (8-plex iTRAQ) and tandem mass spectrometry (MS/MS) were used to identify differentially expressed protein markers of CCA using animal and human models of CCA. In the hamster model of Ov-induced CCA, protein expression levels in the livers from Ov-infected hamsters that had progressed to CCA were compared with normal uninfected hamsters as well as to hamsters that were "Ov-infected" but did not receive NDMA and were thus CCA-free (Fig. 1). Specifically, we attempted to identify protein markers of CCA that were distinct from those associated with the strong inflammation caused by Ov infection; that is, differentially expressed proteins that were either (1) associated with Ov-induced CCA but not Ov-associated inflammation when compared with normal controls, or (2) proteins associated with both inflammation and CCA but which exhibited significantly different expression in Ov-induced CCA when compared with Ov-associated inflammation. To verify these observations in human Ov-associated CCA, immunoblotting experiments and immunohistochemical analysis of CCA tissue microarrays (TMAs) were also assayed for the expression levels for these dysregulated proteins. The results of this study provide protein "signatures" of both Ov-associated inflammation and Ov-associated CCA that can be further exploited for clinical application as well as insight into the relationship between Ov-associated chronic inflammation and Ov-associated CCA.

EXPERIMENTAL PROCEDURES

Experimental Design and Statistical Rationale—Quantitative 8-plex iTRAQ experiments were conducted on whole liver protein preparations from three groups of hamsters: "Normal," "Ov-induced CCA," and "Ov-infected" groups using three biological replicates from each group. Four 8-plex iTRAQ channels were used in each experiment which included two labeled control samples as an internal control; two additional channels were used for a separate study on the effects of curcumin on CCA and Ov infection (see supplemental Table S1 for details of iTRAQ labeling). For verification in hamster liver tissue Western blotting experiments and immunohistochemical analysis were performed using four biological replicates from each of the three experimental groups. All human CCA tissue was obtained with informed consent from patients at Srinagarind Hospital, Khon Kaen University, Thailand. For Western blotting experiments in human CCA tissue, seven biological replicates were used and in each replicate adjacent nontumor tissue was used as a control. Candidate proteins were further verified using IHC analysis on a TMA containing tissue from 68 CCA patients, 48 male and 20 female. The aim of this study was to identify potential leads for further study and sample numbers were predominantly guided by (1) reagent costs; and (2) sample availability.

Parasite and Animal Tissue—Ov metacercariae were obtained from naturally infected cyprinoid fish in Khon Kaen province, Thailand using established methods (8). In brief, fish were digested with 0.25% pepsin-HCl and metacercariae isolated from the resulting slurry. Metacercariae were examined microscopically, counted and viable cysts were used to infect hamsters (*Mesocricetus auratus*). All animal tissue samples were taken from hamsters used in an immunohistochemical study of Ov-induced CCA described in (8) and approved by the Animal Ethics Committee of Khon Kaen University, Thailand (AEKKU 22/2557). The experimental design is shown in Fig. 1A. Hamsters were maintained at the animal research facility of the Faculty of Medicine, Khon Kaen University using protocols approved by the Khon Kaen University Animal Ethics Committee.

Ov-induced CCA in Syrian Golden Hamsters—Twelve male Syrian golden hamsters (*Mesocricetus auratus*) aged between 4–6 weeks were randomly divided into three groups of four animals: (1) the Normal group, which received a conventional murine diet (CP-SWT,

Thailand); (2) the Ov-induced CCA group, which were infected with 50 Ov metacercariae by oral inoculation and fed the control diet supplemented with NDMA for the first two months of the trial (administered in water available *ad libitum* at 12.5 ppm); and (3) the Ov-infected group, which were infected with 50 Ov metacercariae by oral inoculation and fed the control diet.

Patient Tissue—Human liver tissues were prepared as described in (14). Written informed consent was obtained from 68 CCA patients, 48 male and 20 female, who underwent liver resection at Srinagarind Hospital, Khon Kaen University, Thailand between 1999–2010 (HE571283). Patients had a mean age in years of 57 ± 7.7 (38–74 years). The Human Research Ethics Committee, Khon Kaen University, approved the study protocols for obtaining liver samples from the biobank of the Liver Fluke and Cholangiocarcinoma Research Center (HE571294). Frozen liver tissue from seven paired tumor cases (adjacent nontumor and tumor) were used for Western blotting and paraffin-embedded liver tissues from the same cases were used for immunohistochemistry analysis. Tissue microarrays (TMAs) were constructed by the Department of Pathology, Faculty of Medicine, Khon Kaen University as described previously (15). The TMAs contained 68 human CCA cases. To confirm the presence of intact tumor tissue, an H&E stained section of the TMA block was prepared and reviewed by two independent pathologists. Diagnosis of CCA patients was evaluated by clinical data, imaging analysis, tumor markers, and pathology.

Protein Purification from Hamster Livers—Hamster liver tissue (100 mg) from each hamster in each group was suspended in 600 μl of lysis buffer (7 M urea, 2 M thiourea, 4% (w/v) CHAPS and 40 mM Tris-Base) and homogenized with a Microtube Bead Homogenizer at 4 °C for 5 min. The sample was sonicated for 1 min and incubated on ice for 30 min. The solubilized samples were centrifuged at 12,000 × *g* for 20 min at 4 °C. Protein samples were precipitated with 6 volumes of cold acetone at −20 °C overnight. Proteins were then pelleted using centrifugation at 8000 × *g* at 4 °C for 10 min and the pellets resuspended in 0.5 M triethylammonium bicarbonate (TEAB) pH 8.5 (Sigma-Aldrich, Castle Hill, Australia) and 0.1% SDS. Proteins were quantified by Bradford protein assay (Bio-Rad, Gladesville, Australia) using the manufacturer's recommendations.

Reduction, Alkylation and iTRAQ Labeling—Total liver proteins from three biological replicates were analyzed in three 8-plex iTRAQ experiments. Liver proteins (100 μg) from three hamsters in each group were reduced, alkylated, and labeled using the iTRAQ 8PLEX Multiplex Kit (AB SCIEX, Mt Waverley, Australia). Briefly, protein samples were reduced with 10 mM dithiothreitol at 60 °C for 1 h and alkylated in 50 mM iodoacetamide or methyl methanethiosulfonate (MMTS) at 37 °C for 30 min. Proteins were then digested with 2μg of trypsin at 37 °C for 16 h. iTRAQ labeling reagents were prepared by adding 50 μl of isopropanol to each vial and these were then used to label the peptide samples for 2 h at room temperature. Labeled peptides were combined into three mixtures, representing three biological replicates, each containing four peptide samples (Ov-induced CCA, Ov-infected and two control channels). After labeling, peptide mixtures were cleaned using HiTrap ion exchange columns (GE Healthcare, Little Chalfont, UK) and desalted using a Sep-Pak Vac C18 cartridge (Waters, Milford, MA). Cleaned fractions were then lyophilized prior to OFFGEL™.

OGE Fractionation—The 3100 OFFGEL Fractionator and OFFGEL kit pH 3–10 (Agilent Technologies, Santa Clara, CA) with a 24-well setup were prepared using the manufacturer's recommendations. Lyophilized peptide mixtures were diluted to a final volume of 3.6 ml using the OFFGEL peptide sample solution. IPG gel strips (24 cm) with a 3–10 linear pH range (GE Healthcare) were rehydrated with the Peptide IPG Strip Rehydration Solution using the manufacturer's recommendations and 150 μl of sample was loaded in each well. Peptides were isoelectrically focused with a maximum current of 50 μA until 50 kV-h were achieved. Twenty-four fractions were recovered from each well and the wells were rinsed with 150μl of water/methanol/formic acid (49/50/1) for 15 min. Each fraction was lyophilized and then resuspended in 15μl of H_2O with 5% (v/v) formic acid prior to LC-MS/MS analysis.

Isolation and Purification of Exosomes from KKU055 Cell Line—The human CCA cell line KKU055 (moderately differentiated) was cultured in RPMI 1640 (GIBCO, Life Technologies, Waltham, MA) media containing 1% Penicillin-Streptomycin (GIBCO, Life Technologies) and 10% Fetal Calf Serum (GIBCO, Life Technologies) in a 25 cm^2 culture flask (Greiner Bio One, Kremsmünster, Austria) for the first generation. For the second generation heat treated 10% FCS was used. Cell growth was carried out at 37 °C under 5% CO_2 and 95% humidified air. Upon reaching 80% confluency the cells were washed with 1× PBS and trypsinized using 0.25% Trypsin-EDTA (GIBCO, Life Technologies) and pelleted at 800 × *g* for 5 min before they were split into 175 cm^2 culture flask (Greiner Bio One) in equal volumes. Approximately 800 ml of culture supernatant was collected at 80% confluency from each generation of the cell lines. Cell culture supernatants were subjected to differential high-speed centrifugation for isolation of exosomes as follows: the supernatant was centrifuged for 30 min at 2000 × *g*; the supernatant was then transferred to new tubes and centrifuged for 45 min at 15,000 × *g*. The supernatant was then collected and centrifuged at 100,000 × *g* for 18 h in 3.5 25 × 89 mm thin-wall polyallomer tubes (Beckman, Grea) with a SW31Ti Ultracentrifuge rotor. The pellet was then resuspended in PBS, sterile-filtered (0.2 μm) and centrifuged for a further 2 h at 100,000 × *g* in a TLA100.3 Ultracentrifuge rotor. All centrifugation steps were performed at 4 °C in order to maintain exosome stability. The final pellet was resuspended in Dulbecco's PBS (DPBS, Life Technologies, Australia). Isopycnic separation was used to further purify exosomes using sequential ultracentrifugations in an OptiPrep (Sigma-Aldrich) iodixanol gradient as previously described (16). Briefly, after high-speed centrifugations exosome extracts were subjected to a 0.25 M sucrose and iodixanol density gradient (5–40%). Gradients were prepared in Beckman Coulter Polyallomer 14 × 89 mm thin-wall tubes, under sterile conditions. A volume of 200 μl of exosome sample was added to each gradient column and centrifuged for 18 h, at 4 °C and 100,000 × *g* in a SW41Ti Ultracentrifuge rotor. After centrifugation, 12 × 1 ml fractions were collected from each gradient column and diluted 1:3 with DPBS followed by a 2 h centrifugation at 100,000 × *g* in a TLA100.3 Ultracentrifuge rotor. The pellet was then resuspended in 200 μl DPBS and centrifuged for a further 30 min. Finally, the pellet was resuspended in 50 μl of Tris-HCL solution (pH 7.5). Samples were stored at −80 °C (17).

Assessment of Exosome Presence and Purity—Electron microscopy was used to identify fractions containing exosomes and to confirm the purity of exosomes in exosome preparations. A 2 μl aliquot from each of the exosome samples from density gradient fractions in Tris-HCl solution (pH 7.5) was directly adsorbed onto glow-discharged formvar carbon-coated copper grids on SuperFrost slides (Agar Scientific, Stansted, UK) to obtain a monolayer of exosomes for analysis. Each slide was then negatively stained with freshly prepared 2% uranyl acetate in aqueous suspension. Grids were air-dried for 3 min and imaged using a JEM-100CX transmission electron microscope (JEOL, Akishima, Japan) equipped with a thermionic tungsten filament and operated at an acceleration voltage of 100 kV. Digital images were taken with a pixel size of 0.3 nm using an Olympus Morada camera using exposure times between 100 and 400 mS. A NanoSight instrument (Malvern Instruments, Malvern, UK) was used to assess exosome yield from representative exosome preparations, after iodixanol fractionation, using the manufacturer's recommendations. For NanoSight analysis, 5 μl of exosome preparation

was diluted to 1 ml with PBS. This solution was taken from a 50 μl solution that was the result of purifying 72 ml of culture media.

Exosome Protein Purification and SDS-PAGE—Isolated exosomes were resolubilised in 1 ml 1× PBS and centrifuged at 100,000 × *g* for 60 min at 40 °C to pellet the exosomes. The pellet was resuspended in 200 μl of ice cold Exosome Resuspension buffer (Total Exosome RNA and Protein Isolation Kit, Invitrogen, Carlsbad, CA). The sample was incubated for 5–10 min at room temperature to allow the pellet to dissolve. This was followed by gently pipetting of the sample to ensure that the pellet was completely dissolved. Acetone precipitation was carried out by adding 1:5 volume of acetone and incubating overnight at −20 °C. The samples were then centrifuged at 3000 rpm for 15 min at 40 °C. The supernatant was discarded and the pellet was washed again with acetone and centrifuged at 10,000 rpm for 15 min at 40 °C. The pellet was dissolved in 10 μl of laemmli buffer and incubated at 96 °C for 3–5 min. This solution was loaded on the gel against the ladder (Precision Plus Protein™ Dual Color Standards) sequence and subjected to SDS-PAGE and in-gel digestion.

Exosome protein samples (30 μg) were applied to 1-mm-thick 4% stacking, 12% resolving gel for SDS-PAGE. Electrophoresis was carried out at 100 V for 20 min and then 200 V for 50 min. The gels were stained using Coomassie Brilliant Blue and destained in 25:10:65 methanol/acetic acid/water (v/v/v). SDS-PAGE gel lanes were divided into ~24 slices and each slice cut into small pieces. Each gel slice was processed independently and was firstly destained twice by incubation in 50% acetonitrile, 200 mM NH_4HCO_3 for 45 min at 37 °C and then dried using a vacuum centrifuge. The gel pieces were resuspended in 20 mM dithiothreitol (DTT) and reduced for 1 h at 65 °C. DTT was removed, and the samples alkylated by the addition of 50 mM iodoacetamide and incubation in darkness at 37 °C for 40 min. Gel pieces were washed twice in 25 mM NH_4HCO_3 for 15 min and completely dried in a vacuum centrifuge. Gel pieces were rehydrated with 20 μl of trypsin reaction buffer (40 mM NH_4HCO_3, 10% acetonitrile) containing 20 μg/ml trypsin (Sigma) for 20 min at room temperature. An additional 50 μl of trypsin reaction buffer was added to the samples and incubated overnight at 37 °C. The digest supernatant was removed from the gel slices, and residual peptides were washed from the gel slices by incubating three times with 0.1% formic acid for 45 min at 37 °C. The original supernatant and extracts were combined and dried in a vacuum centrifuge. The tryptic peptides were resuspended in 12 μl 5% formic acid before mass spectral analysis.

Tandem Mass Spectrometry—Labeled peptides from iTRAQ experiments and tryptic peptides from in-gel digests of exosome proteins were analyzed by LC-MS/MS on a Shimadzu Prominance Nano HPLC (Shimadzu, Brisbane, Australia) coupled to a Triple TOF 5600 mass spectrometer (AB SCIEX) equipped with a nano electrospray ion source. Two μl of peptide sample (~1.5 μg of protein for iTRAQ experiments) was injected onto a 50 mm × 300 μm C18 trap column (Agilent) at 20 μl/min. The samples were de-salted on the trap column for 5 min using 0.1% formic acid (aq) at 20 μl/min. The trap column was then placed in-line with the analytical nano-HPLC column (150 mm × 75 μm C18, 5 μm, Vydav, Theale, UK) for mass spectrometry analysis. A linear gradient of 1–40% solvent B (90/10 acetonitrile/0.1% formic acid (aq)) over 120 min at 800 nL/minute flow rate, followed by a steeper gradient from 40% to 80% solvent B in 5 min, was used for peptide elution. The ionspray voltage was set to 2000V, declustering potential 100V, curtain gas flow 25, nebuliser gas 1 (GS1) 10 and interface heater at 150 °C. 500 ms full scan TOF-MS data was acquired followed by 20 × 50 ms full scan product ion data in an Information Dependent Acquisition (IDA) mode. Full scan TOF-MS data was acquired over the mass range 350–1800 and for product ions 100–1800. Ions observed in the TOF-MS scan exceeding a threshold of 100 counts and a charge state of +2 to +5 were set to trigger the acquisition of product ion spectra for a maximum of 20 of the most intense ions. The data was acquired and processed using Analyst TF 1.5.1 software (AB SCIEX). The MS proteomics data have been deposited to the ProteomeXchange Consortium (http://proteomecentral.proteomexchange.org) via the MassIVE partner repository (18) with the data set identifier PXD002818.

Spectral Searches and Bioinformatic Analysis—For 8-plex iTRAQ analyses, searches were performed using ProteinPilot v4 (AB SCIEX, Framingham, MA) using the following parameters: allowing for methionine oxidation as a variable modification, carbamidomethylation (or modification with MMTS where appropriate) as a fixed modification, two missed cleavages, charge states +2, +3 and +4 and trypsin as the enzyme. Because of the lack of protein sequences for *M. auratus* searches were conducted against the Uniprot *C. griseus* (golden hamster) proteome data set (UP000001075) as of Oct 2013 (23,878 entries). To assess the level of similarity between the two species the 960 *M. auratus* proteins in SwissProt were compared with their corresponding *C. griseus* protein using BLASTp and an average identity of 84% was determined. Proteins were grouped using ProteinPilot's ProGroup algorithm, single peptide identifications were not considered and only proteins containing at least one unique, significant peptide identification were reported. Searches were also conducted with X! TANDEM Jackhammer TPP (2013.06.15.1) (19) using the same database appended with reversed sequences with the following parameters: enzyme = trypsin; precursor ion mass tolerance = ±0.1 Da; fragment ion tolerance = ±0.1 Da; fixed modifications = carbamidomethylation (or modification with MMTS where appropriate) and 8-plex iTRAQ modification of Lys and N-term free-amines (using modification masses 304.205360 and 304.199040 corresponding to the 297.2 Da mass of the label, $C_{14}N_4O_3H_{25}$, plus the mass of the reporter ions); variable modifications = methionine oxidation and variable labeling of Tyr residues with 8-plex iTRAQ reagents; number of missed cleavages allowed = 2; allowed charge states = +2–+4; and k-score as the scoring algorithm. The Trans Proteomic Pipeline (TPP) (19) was used to validate peptide and protein identifications using PeptideProphet (20) and ProteinProphet (21) and Mayu (22) was used for false discovery rate (FDR) estimation. Using the TPP and the same parameters, with the exception of Lys and N-terminal modification by iTRAQ reagent specified as a variable modification, further searches were conducted to estimate the iTRAQ labeling efficiency. GO enrichment was performed using the BiNGO plugin (23) in Cytoscape (24). Hamster proteins were mapped to their corresponding mouse protein using BLASTp and BiNGO used to identify enriched GO terms using the *Mus musculus* annotations and default parameters. iTRAQ reporter ion intensities from peptides identified by ProteinPilot as suitable for quantitation and which possessed a probability greater than 0.95 (supplemental Table S7) were used in the R package iQuantitator (25) to generate credible intervals for protein expression differences in specific samples. Filtering of peptides for quantitation included the removal of any peptide without the "auto" annotation, including those peptides with "auto - shared MS/MS" providing a set of peptides uniquely assigned to protein identifications. iQuantitator uses a model-based approach to describe variation in observed data and Bayesian inference to estimate credible intervals for protein expression across multiple iTRAQ experiments and proteins were considered up, or down regulated if the start and end of computed 95% credible intervals were >1, or <1 respectively. Only proteins quantified on the basis of two significant peptides were considered. All data and search results were submitted to ProteomeXchange with the accession number PXD002818. Spectral data from the analysis of exosome proteins were searched against the UniProt human proteome database (as of the 1st of February, 2016; 70,611 sequences) using the TPP as described above but without iTRAQ labeling specified as modifications. To determine which exosome proteins were homologous to hamster proteins identified as

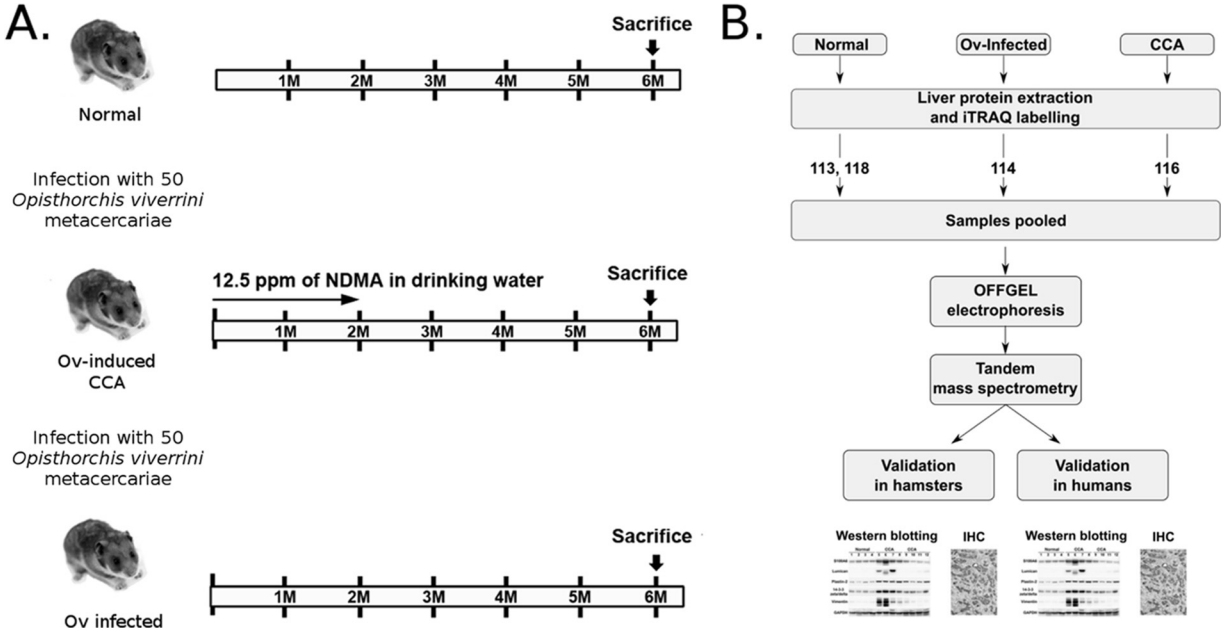

FIG. 1. **Workflow used to identify potential markers for cholangiocarcinoma.** *A*, A hamster model of CCA was used to identify dysregulated proteins in hamsters with Ov-induced CCA and in hamsters infected with Ov ("inflammed" state). To cause experimental Ov-induced CCA (the "Ovinduced CCA" group), hamsters were infected with Ov metacercariae and had their diet supplemented with NDMA. The "Ov-infected" group were infected with Ov but received no NDMA; *B*, Hamster livers were resected and iTRAQ and tandem mass spectrometry used to profile protein expression levels. Antibodies for five proteins were then used to validate iTRAQ findings in both hamster and human tissue using immunoblotting and immunohistochemistry.

significantly dysregulated, the "blastp" program was used to search human proteins against a database of hamster proteins with a bt score cutoff of 50.

Western Blotting—For immunoblotting of hamster and human liver tissue, 120 mg of liver tissue was minced and incubated on ice for 30 min in ice-cold lysis buffer after which the protein concentration was determined using the Bradford assay. Ten micrograms of liver protein was separated on a 12% SDS-PAGE gel and transferred to a polyvinylidene difluoride membrane (PVDF, Amersham Bioscience, Piscataway, NJ) for 2 h at 60 V. The membrane was incubated overnight at 4 °C with primary antibody, diluted in 2% nonfat dried milk/1X Phosphate Buffered Saline Tween-20 (PBST). The membrane was then incubated with the appropriate horseradish peroxidase-conjugated secondary antibody (1:3000, GE healthcare) diluted in 2% nonfat dried milk/PBST and visualized by enhanced chemiluminescence using ECL Western blotting Detection Reagent (GE Healthcare). The ImageQuant TL software v2005 (1.1.0.1) (Nonlinear Dynamics, Durham, NC) was used for quantitative analysis of each band. The relative band intensity of the treated group was normalized by average normal control to adjust for experimental variation.

Immunohistochemistry and Scoring—Hamster tissue ($n = 4$ from each group), human paired tumor and distal normal tissue ($n = 7$) and human TMAs ($n = 68$) were cut into 5-μm sections and mounted on silane-coated slides (Sigma-Aldrich) using the immunoperoxidase method (26). Sections were deparaffinized in xylene and hydrated in graded alcohols. For antigen retrieval, slides were floated on 10 mM citric acid buffer (pH 7.0) and heated for 10 min at 110 °C and allowed to cool. Slides were washed and blocked for endogenous peroxidase in 3% hydrogen peroxide diluted in PBS for 15 min. After washing with PBS, sections were blocked with 5% fetal bovine serum for 30 min and then incubated at 4 °C overnight with primary antibodies. Sections were washed with PBS and incubated with the appropriate secondary antibodies for 30 min at room temperature. Sections were then developed with 3,3′-diaminobenzidine (DAB; Sigma-Aldrich), counter-stained with Mayer hematoxylin and mounted in Permount. The staining density and intensity in hamster tissue was scored as described previously (27). Briefly, the intensity of protein expression was graded as follows: 0, no staining; 1+, mild; 2+, moderate; and 3+, strong. The staining density was quantified as the percentage of cells stained positively in tissue as follows: 0, no staining; 1, positive staining in $<$25%; 2, 25–50%; and 3, $>$50%. The intensity score was multiplied by the density score to yield an overall score of 0–9 for each sample. For hamster tissue, all sections were evaluated by three investigators, blinded to grading in hamster sections, and when there was consensus between two of the three investigators this grade was designated as acceptable. For human tumor tissue in TMA experiments, 68 cases provided triplicate tissue spots and positive areas were categorized as follows: negative ($<$10%) and positive ($\geq$10%) as described previously (28). As described above, all sections were evaluated by three investigators blinded to grading and the consensus of two from three investigators was designated an acceptable grade.

Statistical Analyses—In Western blot analysis protein expression levels in each group were compared and statistical significance of band intensity was assessed using the Student's *t* test and the data expressed as mean ± S.D. For statistical analysis of IHC experiments in hamster tissue a nonparametric Mann-Whitney *U* test was used to compare the IHC expression level of each protein. Statistical analyses were performed using SPSS version 15 (SPSS, Inc, Chicago, IL). A p value of less than 0.05 was considered statistically significant.

RESULTS

O. viverrini Induced CCA in Hamsters—The experimental design is set out in Fig. 1*A*; briefly, three groups each consisting of four hamsters ($n = 4$) were maintained for six

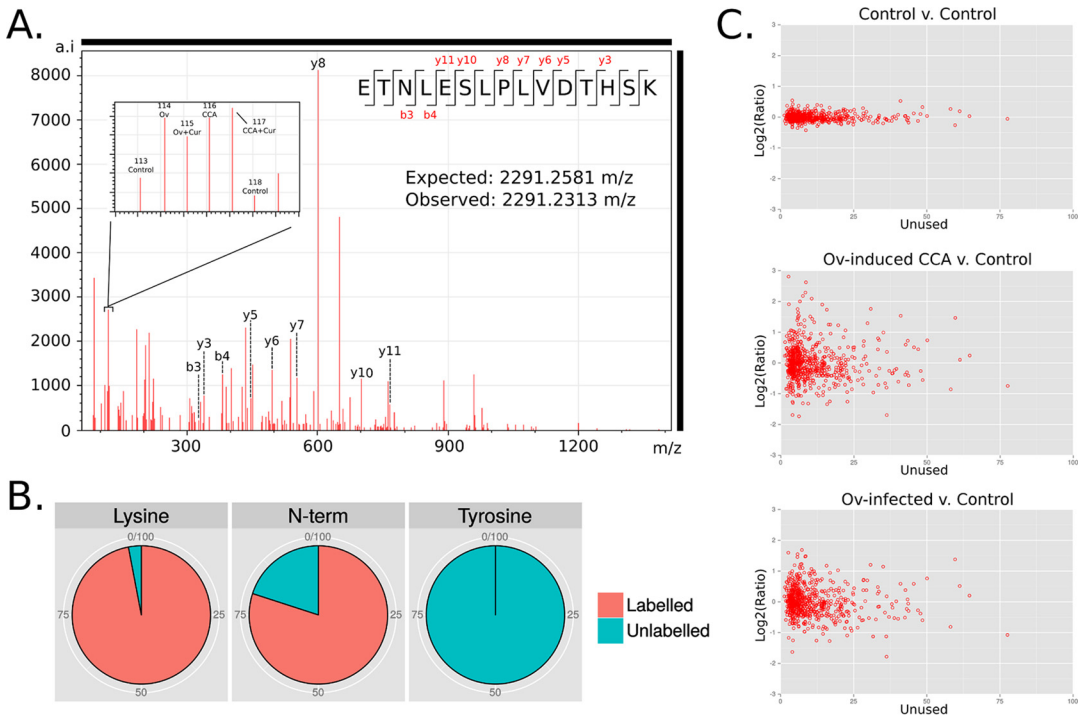

FIG. 2. **Isobaric labeling (iTRAQ) of hamster liver proteins.** *A*, Representative spectrum from tandem mass spectrometry of hamster liver proteins with reporter ions used for quantitation (inset); *B*, Labeling efficiency was assessed using searches specifying iTRAQ labels as variable modifications; *C*, In each iTRAQ replicate two aliquots of the same control sample were labeled with different reporter ions and used as internal validation of expression ratios.

months as follows: an Ov-induced CCA group with hamsters proceeding to Ov-induced CCA (*i.e.* diet supplemented with NDMA); an Ov-infected group, with hamsters infected with Ov but without CCA (*i.e.* diet not supplemented with NDMA); and a Normal group with hamsters without Ov-infection or Ov-induced CCA. For 8-plex iTRAQ experiments, total protein from livers from three hamsters in each group were used as biological replicates (Fig. 1*B*).

Quantification of Protein Expression in Hamster Livers—Trypsinized and isobarically labeled total hamster liver protein, in triplicate, was fractionated using OFFGEL electrophoresis (OGE) and subjected to tandem mass spectrometry. ProteinPilot searches of the UniProt hamster proteome database identified 904 proteins with at least two significant peptides and an Unused score $> = 2.3$ (corresponding to a p value cutoff of <0.01) (supplemental Table S2*A*). Local false discovery rates, calculated using the nonlinear fitting method [29], were below 1% for each replicate. Similar results were obtained (769 identified proteins; at least two unique peptides and a FDR of < 0.01) using the TPP and Mayu for FDR estimation (supplemental Table S2*B*). The 8-plex iTRAQ reporter ions from each label were used to quantitate protein levels in the experimental groups (for an example spectra see Fig. 2*A*). Labeling efficiency was assessed in searches conducted using 8plex iTRAQ labeling as a variable modification and 96% of Lys residues in peptides confidently ($p < 0.05$) assigned to proteins were modified with an iTRAQ label. Approximately 80% of the N termini were labeled, the lower percentage most likely because of N-terminal modification or blocking and/or peptide degradation after labeling (30). Peptides with iTRAQ labeled Tyr residues accounted for only 0.02% of identified peptides and these were excluded from quantitative calculations (Fig. 2*B*). The comparison of the two control channels showed that 95% of the identified proteins had expression ratios within 1.2 and 0.86 whereas control *versus* test samples exhibited much greater variation (Fig. 2*C*).

Proteins Dysregulated During Ov Infection and Ov-Induced CCA—The program iQuantitator (25) was used to identify significantly dysregulated proteins in the Ov induced CCA and Ov-infected groups compared with the Normal group. In the Ov-induced CCA group 246 proteins (137 underexpressed and 109 over-expressed) were dysregulated and, in the Ov-infected group, 121 proteins (69 underexpressed proteins and 52 over-expressed) were dysregulated. A comparison of dysregulated proteins in these two groups further showed that 92 proteins were significantly dysregulated in both the Ov-induced CCA and the Ov-infected groups when compared with the Normal group, whereas 154 proteins were dysregulated only in the Ov-induced CCA group and 29 were significantly dysregulated only in the Ov-infected group (Fig. 3, supplemental Tables S3 and S4). GO enrichment analysis of proteins dysregulated in the Ov-induced CCA group showed enrichment ($p < 0.05$) for metabolic and catabolic "biological process" terms typically associated with cancer, including

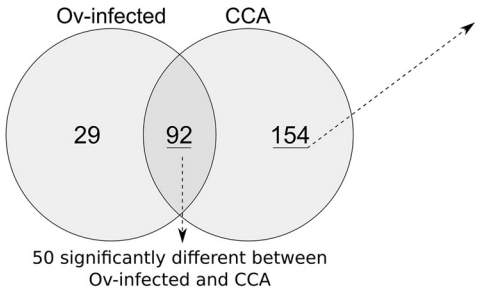

Accession	Unused	SC	Expr. CCA	Expr. Ov Infected	Description
G3HJG6	5.03	3	4.00	1.74	Decorin
G3HC31	7.53	5	4.52	2.19	Protein S100-A6
G3HHR3	26.78	19	3.38	2.38	Vimentin
G3IG05	8.55	4	3.32	1.73	Annexin A1
G3HKZ1	5.25	11	1.98	1.35	14-3-3 protein zeta/delta
G3H8N1	4.19	3	2.62	1.38	Plastin-2
G3HJG5	6.18	5	2.89	3.65	Lumican
G3I4Z7	5.77	3	3.11	1.43	Galectin-1
G3IDD4	6.03	3	2.50	1.31	Serpin H1
G3IH46	6.85	6	2.40	1.46	Prothymosin alpha
G3HRN0	43.75	41	0.61	0.73	ATP synthase subunit beta
G3H2Q4	27.16	29	0.31	0.78	Carbonic anhydrase 3
G3H4W9	44.49	23	0.61	0.91	Carbamoyl-phosphate synthase
G3IGI0	7.52	5	0.40	0.73	60S ribosomal protein
G3HQI8	28.96	18	0.75	0.84	Myosin-Vb

Accession	Unused	SC	Expr. CCA	Expr. Ov Infected	Description
G3IMT4	9.39	10	0.62	0.95	Alcohol dehydrogenase 1
G3IH96	3.29	2	0.58	0.80	Eukaryotic translation initiation factor 4B
G3H2K2	6.32	7	0.61	0.78	Cytochrome c
G3I1V3	16.99	9	2.08	1.07	Fibronectin
G3HRM4	15.96	10	0.74	0.97	Retinol dehydrogenase 2
G3IG06	12.22	8	0.75	0.95	Sarcosine dehydrogenase
G3GV35	6.80	4	0.71	0.89	3-hydroxyanthranilate 3,4-dioxygenase
G3HNK4	2.77	2	1.71	1.22	Dihydropyrimidinase-related protein 2
G3IDU6	6.00	3	0.76	0.94	Argininosuccinate lyase
G3H2J8	16.71	15	0.71	1.10	Nuclear ribonucleoproteins A2/B1
G3HED9	4.73	5	0.56	0.75	ATP synthase subunit e
G3GYT9	5.83	4	0.67	0.84	Cytochrome P450 4A14
G3H284	3.73	3	0.70	0.87	Endoplasmic reticulum protein Erp29
G3I071	2.61	2	0.61	0.80	60S ribosomal protein L35
G3GZX4	2.99	2	0.69	0.79	Dihydrodipicolinate synthase-like
G3HSL4	4.13	3	1.28	0.92	Elongation factor 2
G3HKG9	4.12	3	1.26	1.14	60S acidic ribosomal protein P0
G3GSJ7	5.04	2	0.77	1.09	D-beta-hydroxybutyrate dehydrogenase
G3I0Q0	11.71	6	1.18	1.09	Non-muscle caldesmon
G3HYJ9	2.22	2	2.01	1.34	Moesin
G3HY04	5.55	5	1.40	1.10	Glutathione S-transferase theta-1
G3IA94	10.33	6	1.94	1.17	Myosin regulatory light chain 12B
G3I6I6	14.50	10	1.78	1.19	Tubulin alpha-1A chain
G3HDE5	18.11	13	0.63	0.94	Proteasome activator complex subunit 1
G3I4W7	3.44	3	2.09	1.17	Cathepsin D
G3HMV6	6.15	6	0.57	0.89	Hydroxymethylglutaryl-CoA lyase
G3I3H2	5.61	7	0.68	0.79	60S acidic ribosomal protein P2
G3I4W0	9.21	8	0.80	0.90	Acyl-coenzyme A oxidase
G3GZD2	6.18	3	0.83	1.01	Phosphoglucomutase-1
G3H5I7	13.21	7	1.41	1.05	Fibrinogen alpha chain
G3ICM8	4.23	16	0.70	0.94	Hemoglobin subunit epsilon-Y2
G3IEB1	6.34	4	2.09	1.29	Annexin
G3H4I2	3.19	12	1.68	0.91	Tropomyosin beta chain

FIG. 3. **Dysregulated proteins common to CCA and Ov-infected group.** Selected proteins identified as dysregulated in the livers of hamsters with experimentally-induced CCA and hamsters infected with Ov. Abbreviations used: Unused — ProteinPilot score for protein identification; SC — number of unique peptides used for protein identification; Expr. CCA — fold-change of protein when compared with normal control sample; Expr. Ov infected — relative fold-change when compared with normal control sample.

organonitrogen compound biosynthetic processes and the metabolism and catabolism of hydrogen peroxide, as well as terms related to the response to "wound healing" and "cell-cell adhesion" (supplemental Table S5*A*). GO enrichment analysis of protein dysregulated in the Ov-infected group showed a very similar profile of enriched "biological processes" with all 40 terms enriched in this group also enriched in the Ov-induced CCA group (supplemental Table S5*B*). Of the 92 proteins identified as dysregulated in both the Ov-infected and Ov-induced CCA groups, when compared with the Normal group, all exhibited a pattern of expression in which the Ov-induced CCA group showed the greatest magnitude of dysregulation when compared with the Ov-infected group. When the Ov-induced CCA and Ov-infected groups were directly compared, 165 proteins were identified as dysregulated (77 down-regulated and 89 up-regulated; Suppl. Table 3c), including 50 of the 92 proteins that had been identified as dysregulated in both experimental groups when compared with the normal controls (supplemental Table S6). Many of these 50 proteins, for example vimentin and annexin A1 (31), have been associated with different malignancies which, when combined with the very similar enriched GO terms from the Ov-induced CCA and Ov-infected groups, suggests that some protein expression changes associated with cancer are occurring during infection and that increased expression of these proteins could mark the transition from infection to CCA.

Validation of iTRAQ Data in Hamster Tissue—To provide an independent measure of protein expression in hamster tissue five proteins were selected for immunohistochemistry (IHC) and immunoblotting experiments on the basis of 1) the significance (*p* value) and magnitude (expression ratio) of their dysregulation and 2) the functional significance of the protein. In the Ov-induced CCA group, immunoblotting of five proteins (S100A6, lumican, plastin-2, 14-3-3 zeta/delta and vimentin) exhibited the same expression profile observed in 8-plex iTRAQ experiments (Fig. 4*A* and 4*B*). In the Ov-infected group, four proteins (prolargin, plastin-2, 14-3-3 zeta/delta, and vimentin) also exhibited the same expression profile in immunoblotting experiments as was observed in iTRAQ experiments (data not shown). In IHC experiments using graded tumor tissue from the Ov-induced CCA group, expression of S100A6, lumican, plastin-2 and 14-3-3 zeta/delta was observed in the cytoplasm of bile duct tumor, whereas vimentin was found mainly in the cytoplasm of fibroblasts at periductal fibrosis and tumor stroma (Fig. 4*C*). Once again, protein expression mirrored that observed in the iTRAQ experiments (Fig. 4*C* and 4*D*). In evaluating staining density and intensity, three independent investigators provided the same grade for each sample.

Validation of iTRAQ Data Using Immunoblotting and Immunohistochemistry in Human Tissue Tissue—To determine the relevance of the hamster data to human Ov-associated CCA, five proteins (S100A6, lumican, plastin-2, 14-3-3 zeta/delta, vimentin) that were over-expressed in the Ov-induced CCA hamster group were assayed in human CCA cases. Paired tumor and distal normal tissue (*i.e.* tissue taken at a site near the CCA tumor but with no evidence of frank carcinoma or observed dysplasia) from seven human CCA cases were analyzed using immunoblotting (Fig. 5*A*) with the relative band intensity of all proteins shown in Fig. 5*B*. Protein S100A6, 14-3-3 zeta/delta and vimentin were significantly increased in human CCA tumor tissue whereas lumican and plastin-2 were not significantly up-regulated, although there was a trend

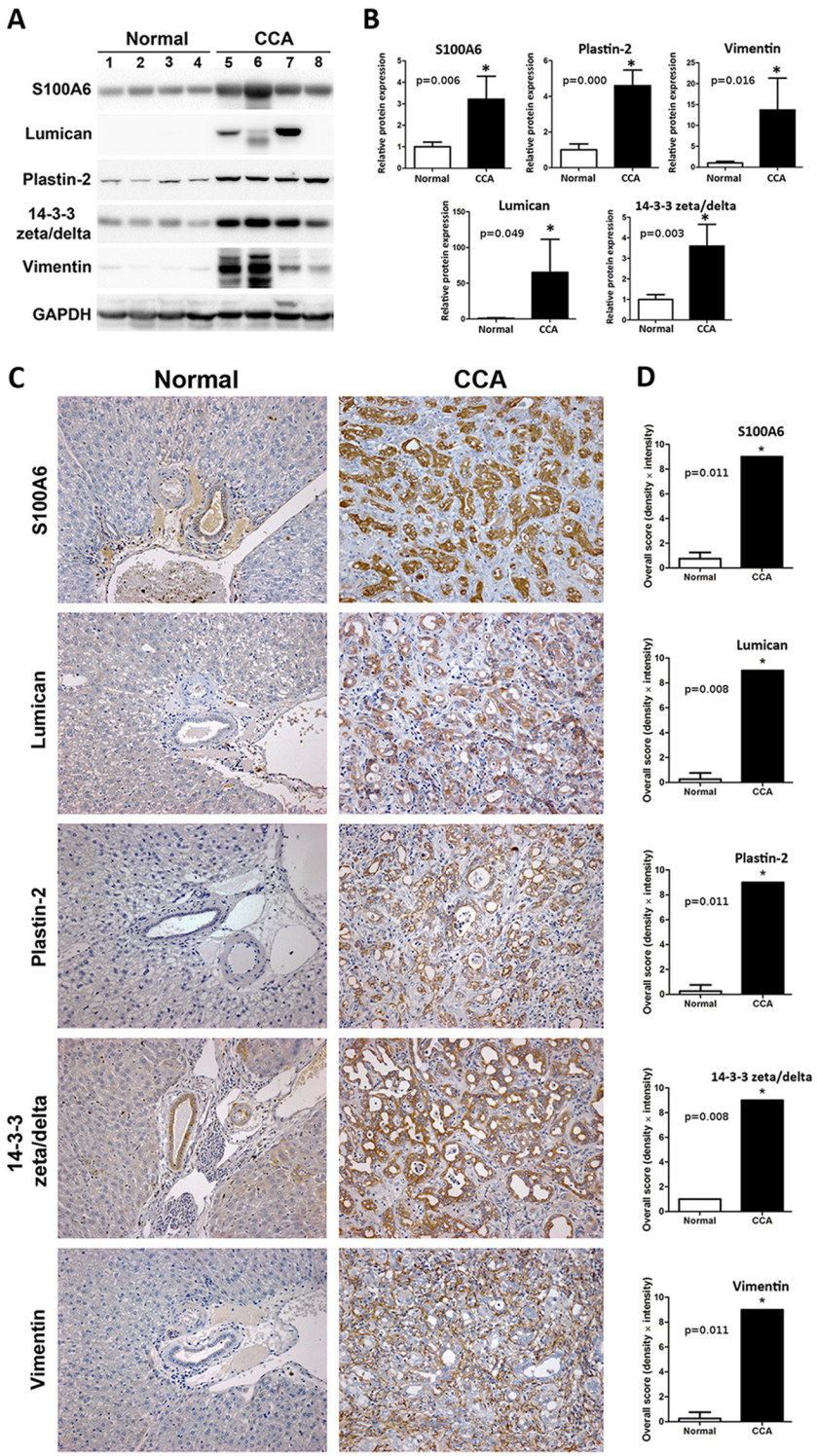

FIG. 4. **Validation of iTRAQ data in hamster tissue.** Expression changes of five proteins (S100A6, lumican, plastin-2, 14-3-3 zeta/delta and vimentin) were evaluated by Western blot and Immunohistochemistry (IHC). *A*, Western blot analysis of candidate proteins in normal (lane 1–4) and "Ov-induced CCA" groups (lane 5–8); *B*, The relative band intensity of the Western blot in the "Ov-induced CCA" group was normalized by the average normal and the results are shown as a bar graph; *C*, A representative immunohistochemistry experiment showing staining of five proteins in hamster livers. The sample shown is representative of each group (4 cases/group; original magnification, ×200); *D*, Protein expression levels were estimated from (*C*) by intensity score and multiplied with the density score to yield an overall grading score. The grading results are shown as a bar graph. In (*B*) and (*D*), asterisk (*) denotes significant difference ($p < 0.05$) by Student's *t* test *versus* normal and significant *p* values are shown on bar plots.

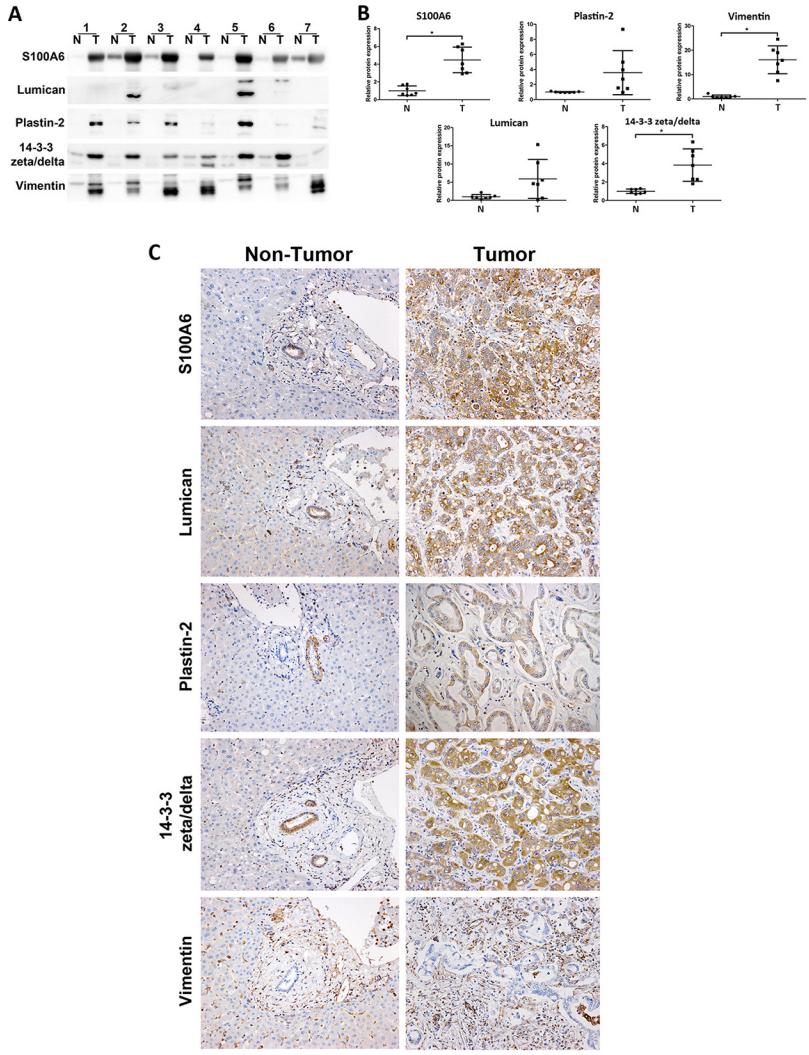

FIG. 5. **Validation of iTRAQ data in human tissue.** Expression changes of five proteins (S100A6, lumican, plastin-2, 14-3-3 zeta/delta and vimentin) were evaluated by Western blot and immunohistochemical staining of human tissue. *A*, Western blot analysis in seven paired tumor cases (N, adjacent nontumor and T, tumor tissue); *B*, the relative band intensities were normalized by average normal and plotted as a scatter plots. Asterisk (*) denotes significant difference ($p < 0.05$) by Student's *t* test *versus* "Normal" group and *p* values are shown on the bar plots; *C*, Immunohistochemical staining of the five proteins in the same human tumor tissue samples showed only minor staining in nontumor tissue (original magnification, ×200).

toward increased expression in the latter two proteins. IHC analysis of the same seven samples showed that, as in the hamster experiments, S100A6, lumican, plastin-2, 14-3-3 zeta/delta were observed in the cytoplasm of bile duct tumor, whereas vimentin was found mainly in the cytoplasm of fibroblasts at periductal fibrosis and tumor stroma (Fig. 5*C*). Tissue adjacent to tumor tissue but with no evidence of frank carcinoma showed only minor staining (Fig. 5*C*) in all seven cases. To examine protein expression in a larger number of samples we used IHC analysis of a human CCA TMA to investigate positive staining of the five proteins used in the immunoblotting experiments in 68 human CCA cases. Positive staining rates in tumor tissues were 78% (53 of 68) for S100A6, 84% (57 of 68) for lumican, 50% (34 of 68) for plastin-2, 82.4% (56 of 68) for 14-3-3 zeta/delta and 98.5% (67 of 68) for vimentin. For TMA experiments 90% of the samples received the same grade from three independent investigators and 10% of the samples had a consensus from at least two of the investigators.

Identification of Potential Circulating Markers for CCA—A number of studies have now established that exosomes secreted by cancer cells can be differentiated on the basis of their protein cargo and that these proteins show cell-type specificity (32). Accordingly, great interest has been shown in exploiting circulating exosomes as biomarkers of disease or as a mechanism for reducing the dynamic range of the circulating proteome (33). In order to identify potential circulating markers of CCA, we characterized the proteome of exosomes secreted by the KKU055 human CCA cancer cell line and compared them to CCA-associated proteins identified in the hamster experiments. Using NanoSight, we determined a

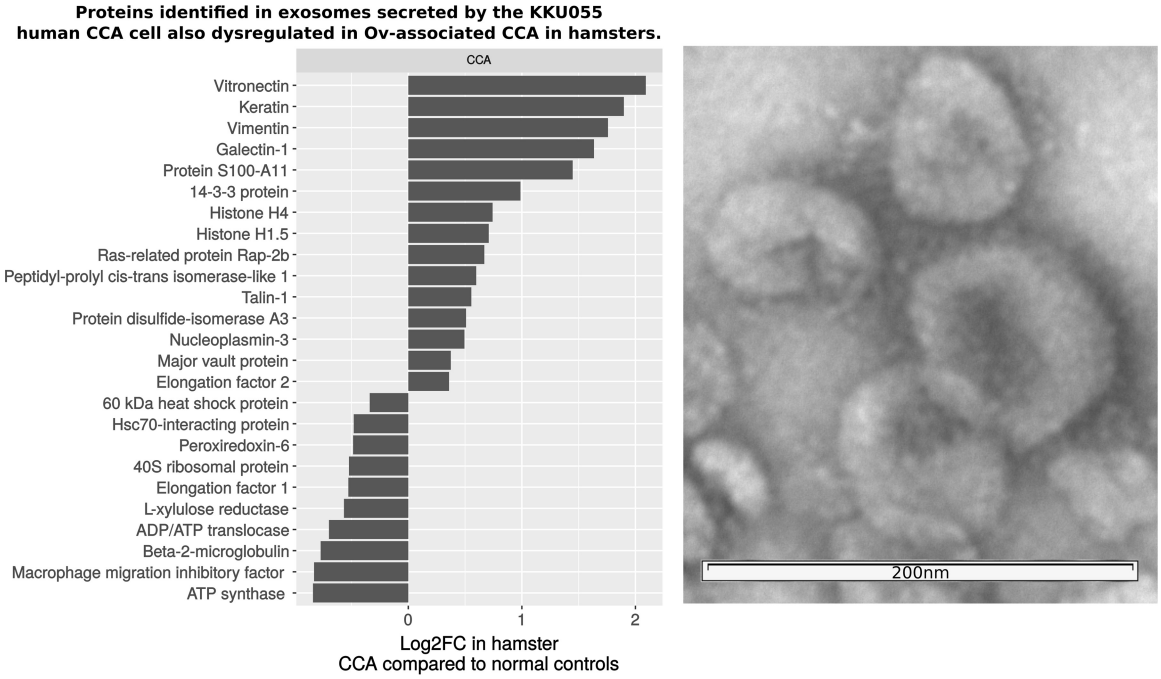

FIG. 6. **Proteins homologous to hamster proteins dysregulated in CCA that were identified in exosomes secreted by the human CCA cell line KKU055.** Twenty-seven human exosomes proteins, from 282 total identifications, were found to be homologous (BLAST bit score >50) to proteins dysregulated in the hamster model of CCA. These included some of the most highly over-expressed proteins in hamster livers of hamsters with CCA. On the right, transmission electron micrograph of exosome preparation used in proteomics experiments.

yield of ~3e6 exosomes per ml of KKU055 culture media using differential centrifugation and density gradient centrifugation (counting particles in the size range of 50 to 120 nm; see supplemental Fig. S1 for NanoSight output from a representative exosome preparation). Tandem mass spectrometry of exosome proteins then provided 282 identifications at a FDR of < 0.01 (each identification comprising of at least two peptides at least one of which was unique; supplemental Table S8). These proteins were compared with proteins significantly dysregulated in the Ov-induced CCA hamster group using BLAST and 27 proteins were found in common (summarized in Fig. 6 and in Suppl. Table IX). These proteins included some of the most highly up-regulated proteins identified in the Ov-induced CCA group, including vimentin, galectin1, vitronectin and Protein S100; two of these, vimentin and protein 14-3-3, were also validated as up-regulated in human immunoblotting and IHC experiments. The presence of these CCA-associated proteins in exosomes secreted by a human CCA cell line suggests that these proteins are important targets for future validation in CCA patients as potential diagnostic and/or prognostic protein markers.

DISCUSSION

Ov-associated CCA presents an exceptional model for investigating the role of inflammation-associated cancers, as it progresses through a series of well-defined clinical stages that can be detected in both a human and animal model. Moreover, the chronic inflammation during Ov infection, which can last for years, has been shown to have an etiologic role in the development of Ov-associated CCA in the human and animal models of this bile duct cancer. The pattern of protein expression in the Ov-infected and Ov-induced CCA hamsters groups showed protein dysregulation profiles that could discriminate between the subclinical and clinical stages leading to Ov-associated CCA. Protein markers that could discriminate between Ov infection and Ov-associated CCA are of particular interest in areas where Ov is endemic and the prevalence of Ov infection rates can reach as high as 75% of the population (4). In our previous work, we have shown that systemic and Ov-specific interleukin-6, a known inflammatory cytokine, are associated with Ov-associated CCA and that this cytokine possesses a positive association with advanced periductal fibrosis, a precursor stage to CCA and to Ov-associated CCA itself (34). However, the low diagnostic specificity of IL-6, which has been proposed as a inflammatory marker for many conditions (*e.g.* cancer (35), mechanical injury (36) and bacterial infection (37) among others) decreases its utility as a diagnostic marker for CCA. Proteins in clinical use as markers of Ov-associated CCA suffer from a similar lack of diagnostic specificity: *e.g.* the carbohydrate antigen (CA-19-9) is elevated in Ov-associated CCA but also in primary biliary cirrhosis and in individuals who smoke (38). Similarly, the carcinoembryonic antigen (CEA) is elevated in only ~30% of Ov-associated CCA cases. In the current study, we used advanced proteomic techniques (isobaric labeling and tandem mass spectrometry) on animals at the distinct stages

in the transition from Ovinfection to Ov-induced CCA to identify a large number of potential markers for Ov-associated CCA that could also distinguish Ov-associated CCA from the inflammation which accompanies chronic Ov-infection in humans resident in Ov endemic areas and which could be further evaluated for their application as diagnostic markers of CCA.

To identify potential markers for CCA, we identified proteins that were dysregulated in animals with CCA (Ov-induced CCA group) but not during Ov infection (Ov-infected group). Over 150 of these proteins were identified, including many proteins previously associated with cancer. In particular, proteins associated with the extracellular matrix and cell mobility and adhesion were overexpressed in the CCA group, including vitronectin (39), fibronectin (40), septin-7 (41) and talin1 (42) all of which play key roles in the remodeling of the extracellular matrix (ECM), adhesion and metastasis known to occur during human CCA. Likewise, over-expression of Ras-related protein Rap-1b and serum amyloid A protein have been observed as key events during carcinogenesis in several malignancies, the former mediating malignant transformation, proliferation and cell growth (43) and the latter suppressing cell immunity via stimulation of immunosuppressive neutrophils to produce interleukin-10 (44). These proteins were not dysregulated in the Ov-infected group suggesting that proteins associated with these processes can act as markers for the onset of cancer and can discriminate infection from cancer. Likewise, we identified a number of cancer-associated proteins, for example vimentin, lumican and galectin-1, that were already overexpressed during infection, suggesting that some of the key processes that become important during carcinogenesis are active during infection. If changes in the circulating levels of these proteins can be associated with CCA, and both vimentin (45) and galectin-1 (46) were detectable in exosomes from the KKU055 cell line, these proteins could provide useful tools for monitoring infection-related inflammation and, potentially, the transition to CCA.

Ninety-two proteins were dysregulated in both the Ov-infected and Ov-induced CCA groups and the majority of these were shown to be differentially expressed when the Ov-infected and Ovinduced CCA groups were directly compared (Fig. 3) suggesting that processes activated during the inflammatory response continue after transformation to a tumor. In particular, proteins closely associated with the pro-inflammatory transcription factor NF-κB showed dysregulation during infection (Ov-infected group) and a significantly greater magnitude of dysregulation during cancer (Ov-induced CCA group). Activation of NF-κB promotes infiltration of inflammatory cells and alterations to the redox environment. Prolonged activation can induce oxidative DNA damage via constitutive increases in reactive oxygen (ROS) and nitrogen species (NOS). NF-κB activators, *e.g.* clusterin and S100A10, and targets, *e.g.* S100A6, showed increased dysregulation in the Ov-induced CCA group when compared with the Ov-infected group (Fig. 3; supplemental Table S3) as did the downstream targets of S100A6: annexin 2, tropomyosin β, annexin 11 and lamin B1. Similarly, CCA cell lines (KKU100, KKU156 and KKU213) exhibit constitutive activation of NF-κB (47) and the results presented here are consistent with downstream consequences of NF-κB activation. In the context of human Ov infection, decades of sustained injury to the bile duct epithelium by the parasite likely leads to constitutive expression of NF-κB, creating a "smouldering inflammatory milieu" (4, 48) that, ultimately, creates severe hepatobiliary abnormalities, principal among them Ov-associated CCA. Given constitutive activation of NF-κB, protein dysregulation observed in the Ov-induced CCA group could be attributable to differences in the number and/or type of infiltrating immune cells rather than tumor cells. However, IHC of hamster tissue showed predominant cytoplasmic staining of tumor cells for four of the five proteins assayed (Fig. 4), suggesting that tumor cells contribute to the protein dysregulation observed in the Ov-induced CCA group when compared with the Ov-infected group.

On the basis of immunoblotting and IHC experiments, the protein expression profile generated from the hamster model appeared to provide a reasonable approximation of protein expression in the human CCA disease. Three of the five proteins used to verify iTRAQ results in human tissue were found to be significantly over-expressed in immunoblotting experiments and, in IHC experiments on TMA using 68 CCA cases, all but one protein (plastin-2) exhibited increased staining in at least 78% or more of tumors. Thus, not only could the three proteins form the basis of a potential marker for CCA, but these results also suggest that many of the 243 other proteins identified as over-expressed by iTRAQ may also be potential markers for human CCA. In nonendemic regions, no specific and sensitive marker for CCA is in clinical use, as discussed above, CA-19-9 and CEA suffer from a lack of clinical specificity. Several proteins have been associated with CCA in a non-Ov-associated model; both circulating apolipoprotein 1 (49) and vimentin (50) have been associated with CCA and both of these proteins were identified as overexpressed by iTRAQ in this study (supplemental Table S4). One quantitative proteomic study of human non Ov-associated intrahepatic CCA tumor tissue identified 39 dysregulated proteins that are consistent with the dysregulated proteins reported here. Of 16 up-regulated proteins observed in that study, ten proteins were also found to be significantly overexpressed in the current study including, vimentin, protein S100-A11, profilin-1, transgelin-2, prothymosin α, and cofilin (50). Likewise, the overexpression of 14-3-3 zeta/delta has recently been demonstrated in both advanced fibrotic lesions and CCA tissue showing its potential as a marker of risk for Ov-associated CCA (51). Taken together, these similarities suggest that the potential biomarkers identified here will also have utility for the diagnosis of non-Ov-associated CCA.

To be useful, particularly in a resource-poor environment, protein markers need to be detectable in an easily accessible matrix such as blood, urine or saliva. In this work, we used

exosomes from the human CCA cell line KKU055 to determine which CCA-associated proteins are likely to be identifiable in the circulation of CCA patients. Proteins identified in the exosomes included human homologs of the most up-regulated proteins in the hamster model of CCA and key proteins associated with carcinogenesis such as vitronectin, talin-1 and Ras-related protein Rap-1b. These proteins are now being assessed in detail as potential circulating markers of CCA in human patients. As discrete packages of protein and RNA emanating directly from tumor cells, exosomes have a number of advantages when considered as biomarkers: exosomes protect their protein cargo from proteolytic digest; they can be purified from plasma or sera, reducing the dynamic range of this matrix; and previous studies have demonstrated that the number of exosomes in circulation increases in cancer patients (52). Accordingly, exosomes purified from blood and urine are now being assessed as markers for a wide range of malignancies, including prostate (53), lung (54), breast (55), and ovarian cancers (56), among others (33). The work performed in this study now enables a targeted examination of potential protein markers of CCA in exosomes not only from blood but other matrices such as urine and saliva.

In general, cholangiocarcinogenesis is associated with a wide range of cellular changes that are reflected in the protein expression profile of tumor tissue. In the current study, we utilized a robust hamster model of Ov-induced CCA to profile these protein expression profiles using quantitative protein methods, 8-plex iTRAQ labeling and tandem mass spectrometry, to identify potential markers in the transition from Ov-infection to Ov-associated CCA. Using isobaric labeling, we identified over 200 dysregulated proteins that can now inform future efforts to develop a biomarker for the diagnosis of Ov-associated CCA. The over-expression of five proteins was confirmed in hamster tissue and, more importantly, three of these five proteins were then confirmed as over-expressed in human Ovassociated tumor tissue. The latter observation suggests that over-expressed proteins identified in the hamster model of Ov-induced CCA may also be over-expressed in human Ov-associated CCA. Taken together, these data provides a basis for future efforts to develop biomarkers and potential therapeutics for the diagnosis and treatment of Ov-associated CCA as well as other infection-related cancers.

DATA AVAILABILITY

The MS proteomics data have been deposited to the ProteomeXchange Consortium (http://proteomecentral.proteomexchange.org) via the MassIVE partner repository (18) with the data set identifier PXD002818.

* This work was supported by the Higher Education Research Promotion and National Research University Project of Thailand, Office of the Higher Education Commission through the Health Cluster (SHeP-GMS; PD55208 and NRU572004 to JK and SP), Thailand Research Fund through the Royal Golden Jubilee Ph.D. Program, Thailand (JK and SP), award R01CA155297 (JMB and JPM) from the National Cancer Institute, award P50AI098639 (JMB) from the National Institute of Allergy and Infectious Disease and fellowship support (JPM) and research support (JMB and JPM - grant 1051627) from the National Health and Medical Research Council of Australia.

S This article contains supplemental material.

[e] To whom correspondence should be addressed: Department of Infectious Disease, QIMR Berghofer Medical Research Institute, Brisbane, QLD 4006, Australia. Tel.: +61 422 545 745; E-mail addresses: Jason.Mulvenna@qimrberghofer.edu.au.

[f] These authors contributed equally to this work.

REFERENCES

1. Sripa, B., Kaewkes, S., Sithithaworn, P., Mairiang, E., Laha, T., Smout, M., Pairojkul, C., Bhudhisawasdi, V., Tesana, S., Thinkamrop, B., Bethony, J. M., Loukas, A., and Brindley, P. J. (2007) Liver fluke induces cholangiocarcinoma. *PLoS Med.* **4,** e201
2. IARC (1994) Schistosomes, liver flukes and Helicobacter pylori. IARC monographs on the evaluation of carcinogenic risks to humans *IARC monographs on the evaluation of carcinogenic risks to humans* volume 61 pp. 218–221 IARC, Lyon
3. Sripa, B., Bethony, J. M., Sithithaworn, P., Kaewkes, S., Mairiang, E., Loukas, A., Mulvenna, J., Laha, T., Hotez, P. J., and Brindley, P. J. (2011) Opisthorchiasis and Opisthorchis-associated cholangiocarcinoma in Thailand and Laos. *Acta Trop.* **120,** S158–S168
4. Sripa, B., Brindley, P. J., Mulvenna, J., Laha, T., Smout, M. J., Mairiang, E., Bethony, J. M., and Loukas, A. (2012) The tumorigenic liver fluke *Opisthorchis viverrini*–multiple pathways to cancer. *Trends Parasitol.* **28,** 395–407
5. Malhi, H., and Gores, G. J. (2006) Cholangiocarcinoma: modern advances in understanding a deadly old disease. *J. Hepatol.* **45,** 856–867
6. Haswell-Elkins, M. R., Sithithaworn, P., Mairiang, E., Elkins, D. B., Wongratanacheewin, S., Kaewkes, S., and Mairiang, P. (1991) Immune responsiveness and parasite-specific antibody levels in human hepatobiliary disease associated with Opisthorchis viverrini infection. *Clin. Exp. Immunol.* **84,** 213–218
7. Pinlaor, S., Yongvanit, P., Prakobwong, S., Kaewsamut, B., Khoontawad, J., Pinlaor, P., and Hiraku, Y. (2009) Curcumin reduces oxidative and nitrative DNA damage through balancing of oxidant-antioxidant status in hamsters infected with *Opisthorchis viverrini*. *Mol. Nutr. Food Res.* **53,** 1316–1328
8. Prakobwong, S., Yongvanit, P., Hiraku, Y., Pairojkul, C., Sithithaworn, P., Pinlaor, P., and Pinlaor, S. (2010) Involvement of MMP-9 in peribiliary fibrosis and cholangiocarcinogenesis via Rac1-dependent DNA damage in a hamster model. *Int. J. Cancer* **127,** 2576–2587
9. Sheikh, M. Y., Choi, J., Qadri, I., Friedman, J. E., and Sanyal, A. J. (2008) Hepatitis C virus infection: molecular pathways to metabolic syndrome. *Hepatology* **47,** 2127–2133
10. Castello, G., Scala, S., Palmieri, G., Curley, S. A., and Izzo, F. (2010) HCV-related hepatocellular carcinoma: From chronic inflammation to cancer. *Clin. Immunol.* **134,** 237–250
11. Thamavit, W., Bhamarapravati, N., Sahaphong, S., Vajrasthira, S., and Angsubhakorn, S. (1978) Effects of dimethylnitrosamine on induction of cholangiocarcinoma in Opisthorchis viverriniinfected Syrian golden hamsters. *Cancer Res.* **38,** 4634–4639
12. Bhamarapravati, N., Thammavit, W., and Vajrasthira, S. (1978) Liver changes in hamsters infected with a liver fluke of man, *Opisthorchis viverrini*. *Am. J. Trop. Med. Hyg.* **27,** 787–794
13. Chamadol, N., Pairojkul, C., Khuntikeo, N., Laopaiboon, V., Loilome, W., Sithithaworn, P., and Yongvanit, P. (2014) Histological confirmation of periductal fibrosis from ultrasound diagnosis in cholangiocarcinoma patients. *J. Hepatobiliary Pancreat. Sci.* **21,** 316–322
14. Khoontawad, J., Hongsrichan, N., Chamgramol, Y., Pinlaor, P., Wongkham, C., Yongvanit, P., Pairojkul, C., Khuntikeo, N., Roytrakul, S., Boonmars, T., and Pinlaor, S. (2014) Increase of exostosin 1 in plasma as a potential biomarker for opisthorchiasis-associated cholangiocarcinoma. *Tumour Biol.* **35,** 1029–1039
15. Fedor, H. L. and De Marzo, A. M. (2005) Practical methods for tissue microarray construction *Pancreatic Cancer* pp. 89–101 Springer
16. Kalra, H., Adda, C. G., Liem, M., Ang, C. S., Mechler, A., Simpson, R. J., Hulett, M. D., and Mathivanan, S. (2013) Comparative proteomics evaluation of plasma exosome isolation techniques and assessment of the stability of exosomes in normal human blood plasma. *Proteomics* **13,** 3354–3364

17. Théry, C., Amigorena, S., Raposo, G., and Clayton, A. (2006) Isolation and characterization of exosomes from cell culture supernatants and biological fluids. *Curr. Protoc. Cell Biol.* **3,** 3–22
18. Deutsch, E. W., Csordas, A., Sun, Z., Jarnuczak, A., Perez-Riverol, Y., Ternent, T., Campbell, D. S., Bernal-Llinares, M., Okuda, S., Kawano, S., L, M. R., J, C. J., M, W., Ishihama, Y., Bandeira, N., Hermjakob, H., and Vizcaíno, J. A. (2016) The ProteomeXchange consortium in 2017: supporting the cultural change in proteomics public data deposition. *Nucleic Acids Res.* **45,** D1100–D1106
19. Deutsch, E. W., Mendoza, L., Shteynberg, D., Farrah, T., Lam, H., Tasman, N., Sun, Z., Nilsson, E., Pratt, B., Prazen, B., Eng, J. K., Martin, D. B., Nesvizhskii, A. I., and Aebersold, R. (2010) A guided tour of the Trans-Proteomic Pipeline. *Proteomics* **10,** 1150–1159
20. Keller, A., Nesvizhskii, A. I., Kolker, E., and Aebersold, R. (2002) Empirical statistical model to estimate the accuracy of peptide identifications made by MS/MS and database search. *Anal. Chem.* **74,** 5383–5392
21. Nesvizhskii, A. I., Keller, A., Kolker, E., and Aebersold, R. (2003) A statistical model for identifying proteins by tandem mass spectrometry *Anal. Chem.* **75,** 4646–4658
22. Reiter, L., Claassen, M., Schrimpf, S. P., Jovanovic, M., Schmidt, A., Buhmann, J. M., Hengartner, M. O., and Aebersold, R. (2009) Protein identification false discovery rates for very large proteomics data sets generated by tandem mass spectrometry. *Mol. Cell. Proteomics* **8,** 2405–2417
23. Maere, S., Heymans, K., and Kuiper, M. (2005) BiNGO: a Cytoscape plugin to assess overrepresentation of gene ontology categories in biological networks. *Bioinformatics* **21,** 3448–3449
24. Cline, M. S., Smoot, M., Cerami, E., Kuchinsky, A., Landys, N., Workman, C., Christmas, R., Avila-Campilo, I., Creech, M., Gross, B., Hanspers, K., Isserlin, R., Kelley, R., Killcoyne, S., Lotia, S., Maere, S., Morris, J., Ono, K., Pavlovic, V., Pico, A. R., Vailaya, A., Wang, P. L., Adler, A., Conklin, B. R., Hood, L., Kuiper, M., Sander, C., Schmulevich, I., Schwikowski, B., Warner, G. J., Ideker, T., and Bader, G. D. (2007) Integration of biological networks and gene expression data using Cytoscape. *Nat. Protoc.* **2,** 2366–2382
25. Schwacke, J. H., Hill, E. G., Krug, E. L., Comte-Walters, S., and Schey, K. L. (2009) iQuantitator: a tool for protein expression inference using iTRAQ. *BMC Bioinformatics* **10,** 342
26. Prakobwong, S., Khoontawad, J., Yongvanit, P., Pairojkul, C., Hiraku, Y., Sithithaworn, P., Pinlaor, P., Aggarwal, B. B., and Pinlaor, S. (2011) Curcumin decreases cholangiocarcinogenesis in hamsters by suppressing inflammation-mediated molecular events related to multistep carcinogenesis. *Int. J. Cancer* **129,** 88–100
27. Guo, J., Wang, W., Liao, P., Lou, W., Ji, Y., Zhang, C., Wu, J., and Zhang, S. (2009) Identification of serum biomarkers for pancreatic adenocarcinoma by proteomic analysis. *Cancer Sci.* **100,** 2292–2301
28. Yonglitthipagon, P., Pairojkul, C., Chamgramol, Y., Mulvenna, J., and Sripa, B. (2010) Upregulation of annexin A2 in cholangiocarcinoma caused by *Opisthorchis viverrini* and its implication as a prognostic marker. *Int. J. Parasitol.* **40,** 1203–1212
29. Tang, W. H., Shilov, I. V., and Seymour, S. L. (2008) Nonlinear fitting method for determining local false discovery rates from decoy database searches. *J. Proteome Res.* **7,** 3661–3667
30. Unwin, R. D., Griffiths, J. R., and Whetton, A. D. (2010) Simultaneous analysis of relative protein expression levels across multiple samples using iTRAQ isobaric tags with 2D nano LCMS/MS. *Nat. Protoc.* **5,** 1574–1582
31. Hongsrichan, N., Intuyod, K., Pinlaor, P., Khoontawad, J., Yongvanit, P., Wongkham, C., Roytrakul, S., and Pinlaor, S. (2014) Cytokine/chemokine secretion and proteomic identification of upregulated annexin A1 from peripheral blood mononuclear cells cocultured with the liver fluke *Opisthorchis viverrini*. *Infect. Immun.* **82,** 2135–2147
32. Wendler, F., Bota-Rabassedas, N., and Franch-Marro, X. (2013) Cancer becomes wasteful: emerging roles of exosomes in cell-fate determination. *J. Extracell. Vesicles* **2,** 22390
33. An, T., Qin, S., Xu, Y., Tang, Y., Huang, Y., Situ, B., Inal, J. M., and Zheng, L. (2015) Exosomes serve as tumour markers for personalized diagnostics owing to their important role in cancer metastasis. *J. Extracell. Vesicles* **4,** 27522
34. Sripa, B., Thinkhamrop, B., Mairiang, E., Laha, T., Kaewkes, S., Sithithaworn, P., Periago, M. V., Bhudhisawasdi, V., Yonglitthipagon, P., Mulvenna, J., Brindley, P. J., Loukas, A., and Bethony, J. M. (2012) Elevated plasma IL-6 associates with increased risk of advanced fibrosis and cholangiocarcinoma in individuals infected by *Opisthorchis viverrini*. *PLoS Negl. Trop. Dis.* **6,** e1654
35. St John, M. A., Li, Y., Zhou, X., Denny, P., Ho, C. M., Montemagno, C., Shi, W., Qi, F., Wu, B., Sinha, U., Jordan, R., Wolinsky, L., Park, N. H., Liu, H., Abemayor, E., and Wong, D. T. (2004) Interleukin 6 and interleukin 8 as potential biomarkers for oral cavity and oropharyngeal squamous cell carcinoma. *Arch. Otolaryngol. Head Neck Surg.* **130,** 929–935
36. Hergenroeder, G. W., Moore, A. N., McCoy, J. P., Samsel, L., Ward, N. H., Clifton, G. L., and Dash, P. K. (2010) Serum IL-6: a candidate biomarker for intracranial pressure elevation following isolated traumatic brain injury. *J. Neuroinflammation* **7,** 19
37. Singh, P. P. and Goyal, A. (2013) Interleukin-6: a potent biomarker of mycobacterial infection. *Springerplus* **2,** 686
38. Gatto, M., Bragazzi, M. C., Semeraro, R., Napoli, C., Gentile, R., Torrice, A., Gaudio, E., and Alvaro, D. (2010) Cholangiocarcinoma: update and future perspectives. *Dig. Liver Dis.* **42,** 253–60
39. Uhm, J. H., Dooley, N. P., Kyritsis, A. P., Rao, J. S., and Gladson, C. L. (1999) Vitronectin, a glioma-derived extracellular matrix protein, protects tumor cells from apoptotic death. *Clin. Cancer Res.* **5,** 1587–1594
40. Ruoslahti, E. (1999) Fibronectin and its integrin receptors in cancer *Adv. Cancer Res.* **76,** 1–20
41. Russell, S. and Hall, P. (2005) Do septins have a role in cancer? *Br. J. Cancer* **93,** 499–503
42. Lai, M. T., Hua, C. H., Tsai, M. H., Wan, L., Lin, Y. J., Chen, C. M., Chiu, I. W., Chan, C., Tsai, F. J., and Jinn-Chyuan Sheu, J. (2011) Talin-1 overexpression defines high risk for aggressive oral squamous cell carcinoma and promotes cancer metastasis. *J. Pathol.* **224,** 367–376
43. McCormick, F. (1995) Ras-related proteins in signal transduction and growth control *Mol. Reprod. Dev.* **42,** 500–506
44. Moshkovskii, S. A. (2012) Why do cancer cells produce serum amyloid A acute-phase protein? *Biochemistry* **77,** 339–341
45. Satelli, A., and Li, S. (2011) Vimentin in cancer and its potential as a molecular target for cancer therapy *Cell. Mol. Life. Sci.* **68,** 3033–3046
46. Hughes, R. C. (2001) Galectins as modulators of cell adhesion. *Biochimie* **83,** 667–676
47. Prakobwong, S., Gupta, S. C., Kim, J. H., Sung, B., Pinlaor, P., Hiraku, Y., Wongkham, S., Sripa, B., Pinlaor, S., and Aggarwal, B. B. (2011) Curcumin suppresses proliferation and induces apoptosis in human biliary cancer cells through modulation of multiple cell signaling pathways. *Carcinogenesis* **32,** 1372–1380
48. Balkwill, F. R. and Mantovani, A. (2012) Cancer-related inflammation: common themes and therapeutic opportunities. *Semin. Cancer Biol.* **22,** 33–40
49. Wang, X., Dai, S., Zhang, Z., Liu, L., Wang, J., Xiao, X., He, D., and Liu, B. (2009) Characterization of apolipoprotein A-I as a potential biomarker for cholangiocarcinoma. *Eur. J. Cancer Care* **18,** 625–635
50. Dos Santos, A., Court, M., Thiers, V., Sar, S., Guettier, C., Samuel, D., Bréchot, C., Garin, J., Demaugre, F., and Masselon, C. D. (2010) Identification of cellular targets in human intrahepatic cholangiocarcinoma using laser microdissection and accurate mass and time tag proteomics. *Mol. Cell. Proteomics* **9,** 1991–2004
51. *Proteomics Clin. Appl.* **10,** 248–256
52. van der Pol, E., Böing, A. N., Harrison, P., Sturk, A., and Nieuwland, R. (2012) Classification, functions, and clinical relevance of extracellular vesicles. *Pharmacol. Rev.* **64,** 676–705
53. Mitchell, P. S., Parkin, R. K., Kroh, E. M., Fritz, B. R., Wyman, S. K., Pogosova-Agadjanyan, E. L., Peterson, A., Noteboom, J., O'Briant, K. C., Allen, A., Lin, D. W., Urban, N., Drescher, C. W., Knudsen, B. S., Stirewalt, D. L., Gentleman, R., Vessella, R. L., Nelson, P. S., Martin, D. B., and Tewari, M. (2008) Circulating microRNAs as stable blood-based markers for cancer detection. *Proc. Natl. Acad. Sci. U.S.A.* **105,** 10513–10518
54. Li, Y., Zhang, Y., Qiu, F., and Qiu, Z. (2011) Proteomic identification of exosomal LRG1: a potential urinary biomarker for detecting NSCLC. *Electrophoresis* **32,** 1976–1983
55. Rupp, A. K., Rupp, C., Keller, S., Brase, J. C., Ehehalt, R., Fogel, M., Moldenhauer, G., Marmé, F., Sültmann, H., and Altevogt, P. (2011) Loss of EpCAM expression in breast cancer derived serum exosomes: role of proteolytic cleavage. *Gynecol. Oncol.* **122,** 437–446
56. Runz, S., Keller, S., Rupp, C., Stoeck, A., Issa, Y., Koensgen, D., Mustea, A., Sehouli, J., Kristiansen, G., and Altevogt, P. (2007) Malignant ascites-derived exosomes of ovarian carcinoma patients contain CD24 and EpCAM. *Gynecol. Oncol.* **107,** 563–571